

Polarization-based dehazing using two reference objects

Daisuke Miyazaki, Daisuke Akiyama, Masashi Baba,
Ryo Furukawa, Shinsaku Hiura, Naoki Asada,
Hiroshima City University

<http://ime.info.hiroshima-cu.ac.jp/>

Abstract

We propose a polarization-based method to enhance the visibility of an image by canceling the haze effect. Haze is a natural phenomenon that degrades the visibility of a scene. Aerosols in air reflect sunlight and cause polarization. Therefore, we analyze the polarization state of the observed light to remove the haze effect from a captured image. Our approach is to use two reference objects that are known a priori in estimating the parameters of the haze effect. Once the parameters are known, we can improve the image so that the scene is clearly visible. We also present an experimental result using a commercial polarization camera, which can obtain the polarization state of the scene.

1. Introduction

Fog and haze often affect driver safety by reducing visibility, sometimes resulting in serious accidents. Aircraft, trains, and ships can avoid serious accidents by following instructions issued by a control center. By contrast, road vehicles experiencing foggy or hazy conditions are at risk of serious accidents resulting in injury or fatality since third-person guidance is not available. These serious accidents are caused by the delay in recognizing other vehicles and traffic signs due to the lack of visibility. One approach to solving this problem is to improve the visibility of the hazy scene and present a clear scene to drivers without fog and haze.

Recent image processing techniques can cancel out the haze phenomenon. Narasimhan and Nayar [5] first estimated the color vector of air light from the color distribution, then estimated parameters from two images with different densities of haze, and finally removed the haze effect in the image. Tan [10] removed the haze effect in an image using the iterated conditional modes algorithm, where the smoothness term is defined as the smoothness of the neighboring pixel's air light brightness and the data term is defined as the strength of the image edges so that the im-

age edges of the dehazed image are much clearer. Fattal [2] assumed that there is no correlation between the transmission parameter and the surface reflection parameter, and dehazed an image by decorrelating for each 24×24 -pixel window, while weighting the cost function using the chromaticity difference to satisfy the assumption. He *et al.* [3] assumed that an image patch of 15×15 pixels often includes shadow, and they dehazed an image with the understanding that the shadow area only contains the brightness value of the haze. These methods rely on assumptions that might sometimes be physically unreliable.

Polarization [12, 1, 4, 8] is said to be useful in analyzing haze phenomena. Schechner *et al.* [6] estimated the parameters for dehazing using the sky region in an image to enhance the visibility of the image using polarization. Shwartz *et al.* [9] enhanced a hazy image assuming that the wavelet components of the air light and the object reflection are independent. Schechner and Karpel [7] recovered underwater visibility using parameters estimated from the water background region of an image. Treibitz and Schechner [11] actively illuminated a scene under water and enhanced the visibility assuming that the degree of polarization of the object is zero or can be estimated assuming that underwater scattering and object reflection are independent. These methods obtain true results in some cases.

We propose a method that estimates the parameters of haze from the polarization information of two known objects at different distances. The estimated parameters are used to remove the haze effect in the image.

Section 2 explains how the polarization information improves the visibility of the hazy scene, which has been well investigated in existing papers. Section 3 presents our method to estimate the parameters of the haze, and experimental results are presented in Section 4. Finally, we conclude our paper in Section 5 while also discussing the disadvantage of our proposed method.

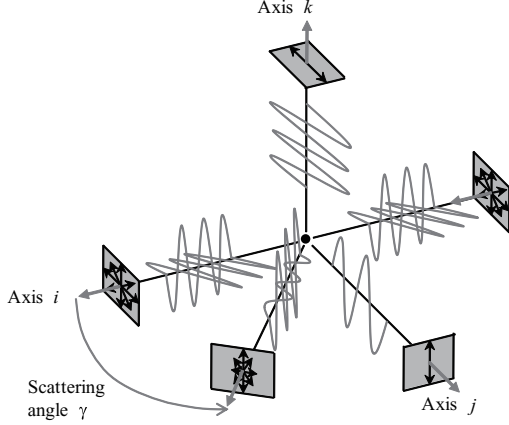


Figure 1. Polarization of the scattered light.

2. Polarization-based dehazing

2.1. Polarization of scattered light

First, we define the plane including the incident light vector and the scattered light vector as the reflection plane. We represent the parallel component of the light with the subscript \parallel , and the perpendicular component of the light with the subscript \perp .

We denote the intensity reflectivity of scattered light as A . The following relationship between the parallel polarization A^{\parallel} and the perpendicular polarization A^{\perp} holds for scattering (Fig. 1).

$$A^{\parallel} \leq A^{\perp} \quad (1)$$

We denote the brightness of scattering as I_s . The parallel and perpendicular components of the scattered light can be expressed as follows.

$$I_s^{\perp} = \frac{A^{\perp}}{A^{\perp} + A^{\parallel}} I_s \quad , \quad (2)$$

$$I_s^{\parallel} = \frac{A^{\parallel}}{A^{\perp} + A^{\parallel}} I_s \quad , \quad (3)$$

$$I_s = I_s^{\perp} + I_s^{\parallel} \quad . \quad (4)$$

If we observe the scattered light through a linear polarizer by rotating it, the maximum brightness I_{\max} is observed when the perpendicular polarization I_s^{\perp} is observed, and the minimum brightness I_{\min} is observed when the parallel polarization I_s^{\parallel} is observed.

The DOP (*or* degree of polarization) is defined as a ratio that takes a value between 0 and 1, where 0 indicates unpolarized light and 1 indicates completely polarized light. When this paper refers to the DOP, it refers to the degree of linear polarization. The DOP ρ of the observed light is defined as follows.

$$\rho = \frac{I_{\max} - I_{\min}}{I_{\max} + I_{\min}} \quad . \quad (5)$$

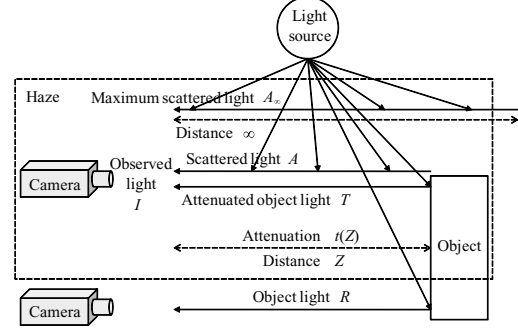


Figure 2. Observation in a hazy scene.

This paper tackles the problem of single-scattered light under a condition of poor visibility. The poor visibility is due to the scattering from aerosols in the atmosphere. The DOP of the scattering is derived from Eq. (2), Eq. (3), and Eq. (5).

$$\rho_s = \frac{A^{\perp} - A^{\parallel}}{A^{\perp} + A^{\parallel}} \quad . \quad (6)$$

2.2. Light reflected from aerosols

Poor visibility of the atmosphere is caused by the scattering of light by particles such as water drops, yellow dust, smoke, and smog. In the case that the density of the particles is high, the light depolarizes and become unpolarized. This paper considers only the single scattering of light by sparsely distributed aerosols, and does not consider the multiple scattering of light, in order to analyze the scattered light with polarizers.

We denote the brightness of the observed light as I , the reflected light of the object attenuated by the haze as T , and the reflected light of the object without attenuation as R . The ratio of attenuation due to the haze is denoted $t(Z)$, where Z denotes the distance between the camera and object. The brightness of the scattered light between the camera and object is denoted A as mentioned before, and the brightness of the scattered light between the camera and an ideally black object located at an infinite distance is denoted A_{∞} . For simplicity, we express A_{∞} as the “maximum scattered light” in this paper. Figure 2 explains the definitions of these terms.

The attenuation of light that penetrates the participating medium is depicted in Fig. 3. Supposing that the radiance of the incident light before penetration is I_0 , and the radiance becomes I_1 after penetrating the medium over a length Z , the following Lambert–Beer law holds.

$$\log \frac{I_1}{I_0} = -\beta Z \quad (7)$$

where β is the optical density. The optical density is the ratio of the attenuation of light, and in this paper, it represents

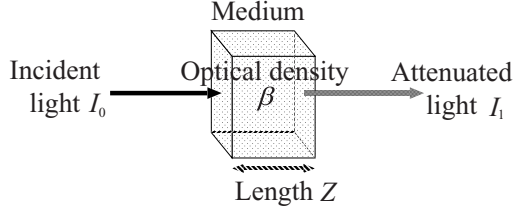


Figure 3. Attenuation.

the density of the haze.

The observed light I under a hazy condition comprises attenuated object light T and the light scattered by aerosols A .

$$I = T + A \quad (8)$$

The attenuation effect of the hazy atmosphere can be expressed as Eq. (9), which is derived from Eq. (7).

$$t(Z) = e^{-\beta Z} \quad (9)$$

The object light R is affected by the attenuation $t(Z)$ and becomes the attenuated light T as follows.

$$T = Rt(Z) \quad (10)$$

Suppose that the brightness of the scattered light for unit length is a . The scattered light is also attenuated by $t(Z)$. In addition, the summation of the scattered light from distance 0 to distance Z is observed as A . Therefore, the scattered light is represented as follows.

$$\begin{aligned} A &= \int_0^Z at(Z)dz \\ &= \frac{a}{\beta} (1 - t(Z)) \end{aligned} \quad (11)$$

Substituting $Z = \infty$ into Eq. (11), the following equation is derived.

$$A_\infty = \frac{a}{\beta} \quad (12)$$

Substituting Eq. (12) into Eq. (11), we derive the following equation.

$$A = A_\infty(1 - t(Z)) \quad (13)$$

2.3. Dehazing

In this section, we explain how to remove haze from an image. This paper assumes that the scene including buildings and vehicles has diffuse reflection, and that the scattered light is polarized by scattering (Fig. 4). Therefore, the parallel and perpendicular components of the observed light, I^\parallel and I^\perp , can be expressed as Eq. (14) and Eq. (15).

$$I^\perp = \frac{T}{2} + A^\perp \quad (14)$$

$$I^\parallel = \frac{T}{2} + A^\parallel \quad (15)$$

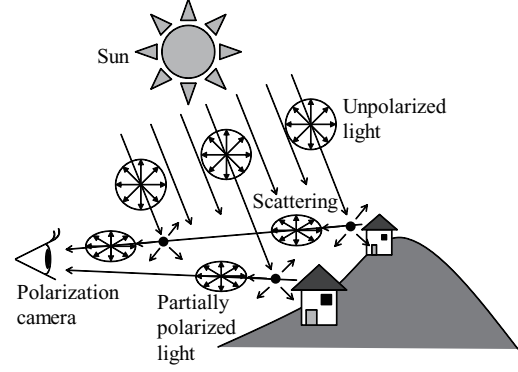


Figure 4. Polarization in the hazy scene.

Note that the parallel and perpendicular components of A and A_∞ have the following relationships.

$$A = A^\perp + A^\parallel \quad (16)$$

$$A_\infty = A_\infty^\perp + A_\infty^\parallel \quad (17)$$

The scattered light is partially polarized, where the perpendicular component of the light is greater than the parallel component. The DOP of the scattered light can be expressed as Eq. (6). Substituting Eq. (13) into Eq. (6), we obtain Eq. (18).

$$\rho_s = \frac{A_\infty^\perp - A_\infty^\parallel}{A_\infty^\perp + A_\infty^\parallel} \quad (18)$$

Consequently, the DOP of the scattered light A can be calculated from the DOP of the maximum scattered light A_∞ , as shown by Eq. (6) and Eq. (18). Substituting Eq. (14), Eq. (15), and Eq. (16) into Eq. (6), the scattered light can be expressed as Eq. (19).

$$A = \frac{I^\perp - I^\parallel}{\rho_s} \quad (19)$$

That is, the scattered light A can be calculated from the observed light I^\perp and I^\parallel , and the DOP ρ_s of the maximum scattered light A_∞ .

Equation (13) can also be expressed as Eq. (20).

$$t(Z) = 1 - \frac{A}{A_\infty} \quad (20)$$

Equation (20) implies that the attenuation coefficient $t(Z)$ can be calculated from the scattered light A and the maximum scattered light A_∞ .

From Eq. (8) and Eq. (10), we obtain Eq. (21).

$$R = \frac{I - A}{t(Z)} \quad (21)$$

As a result, the object light R can be calculated from the scattered light A , the maximum scattered light A_∞ , and the observed light I using Eq. (20) and Eq. (21).

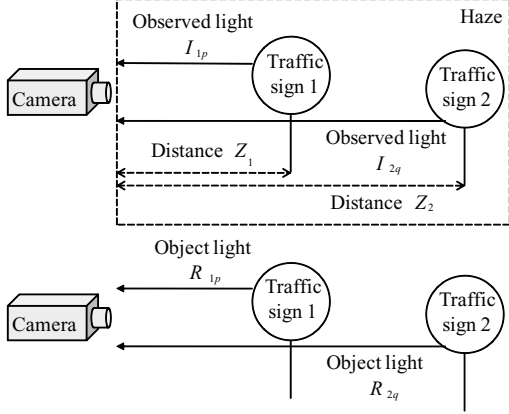


Figure 5. Polarization data for two reference objects.

3. Proposed method

3.1. Parameter estimation

This paper proposes a method to estimate the optical density and maximum scattered light using the polarization information of two objects at different distances. Estimation of the optical density and the maximum scattered light requires polarization information of two objects in a hazy scene and clear scene. This research project supposes the situation that the vehicles are running under conditions of poor visibility; thus, we suppose that we can use traffic signs as the reference objects.

Figure 5 shows the situation what we suppose for estimating the optical density and the maximum scattered light. We denote the observed light of two reference objects under a hazy condition as I_{1p} and I_{2q} , and the observed light of two reference objects under clear sky as R_{1p} and R_{2q} . Here, p and q represent the pixel position of the observed image, and \mathcal{P} and \mathcal{Q} represent the pixel set of each reference object. The parallel and perpendicular components of the observed light of two reference objects are denoted I_{1p}^{\parallel} , I_{1p}^{\perp} , I_{2q}^{\parallel} , and I_{2q}^{\perp} . The distances between the camera and the two reference objects are denoted Z_1 and Z_2 . Table 1 summarizes the notation used in estimating the optical density β and the maximum scattered light A_{∞} .

Substituting Eq. (10) and Eq. (13) into Eq. (8), we obtain the following.

$$I_p^{\perp} - A_{\infty}^{\perp}(1 - e^{-\beta Z_p}) - \frac{R_p e^{-\beta Z_p}}{2} = 0 \quad , \quad (22)$$

$$I_p^{\parallel} - A_{\infty}^{\parallel}(1 - e^{-\beta Z_p}) - \frac{R_p e^{-\beta Z_p}}{2} = 0 \quad . \quad (23)$$

We employ the Levenberg–Marquardt method to estimate the parameters that satisfy Eq. (22) and Eq. (23). Equa-

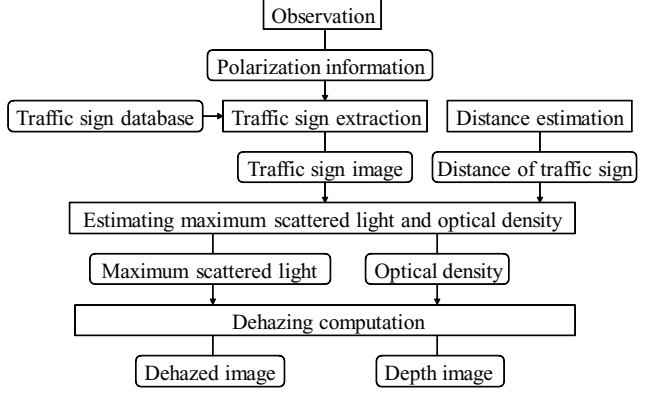


Figure 6. Algorithm flow.

tion (24) is the minimization of the cost function.

$$\{A_{\infty}^{\parallel}, A_{\infty}^{\perp}, \beta\} = \underset{A_{\infty}^{\parallel}, A_{\infty}^{\perp}, \beta}{\operatorname{argmin}} \left[\frac{1}{|\mathcal{P}|} \sum_{p \in \mathcal{P}} \left\{ \left(I_{1p}^{\parallel} - A_{\infty}^{\parallel}(1 - e^{-\beta Z_1}) - \frac{1}{2} R_{1p} e^{-\beta Z_1} \right)^2 + \left(I_{1p}^{\perp} - A_{\infty}^{\perp}(1 - e^{-\beta Z_1}) - \frac{1}{2} R_{1p} e^{-\beta Z_1} \right)^2 \right\} + \frac{1}{|\mathcal{Q}|} \sum_{q \in \mathcal{Q}} \left\{ \left(I_{2q}^{\parallel} - A_{\infty}^{\parallel}(1 - e^{-\beta Z_2}) - \frac{1}{2} R_{2q} e^{-\beta Z_2} \right)^2 + \left(I_{2q}^{\perp} - A_{\infty}^{\perp}(1 - e^{-\beta Z_2}) - \frac{1}{2} R_{2q} e^{-\beta Z_2} \right)^2 \right\} \right]. \quad (24)$$

Our method estimates the maximum scattered light A_{∞} using two traffic images extracted from the database. Since our method is based on principles of physics, the haze effect in the image can be correctly canceled out, which is important for driver safety.

A by-product of implementing our method is that we also obtain the optical density β . The distance to other vehicles, pedestrians, or obstacles can be calculated using the optical density β . The distance can be calculated from the scattered light A_p , the maximum scattered light A_{∞} , and the optical density β . Equation (9) and Eq. (20) are used to derive Eq. (25), which yields the distance.

$$Z_p = -\frac{1}{\beta} \log_e \left(1 - \frac{A_p}{A_{\infty}} \right) \quad (25)$$

3.2. Algorithm flow

The algorithm flow is given in Fig. 6. A standard rectangle in Fig. 6 represents a process whereas a rounded rectangle represents input/output data.

- Image capture of a hazy scene
We captured an image under a poor-visibility condition

Table 1. Parameters for dehazing.

	Observed light (\perp)	Observed light (\parallel)	No haze	Distance	Set of pixels
Traffic sign 1	I_{1p}^{\perp}	I_{1p}^{\parallel}	R_{1p}	Z_1	\mathcal{P}
Traffic sign 2	I_{2q}^{\perp}	I_{2q}^{\parallel}	R_{2q}	Z_2	\mathcal{Q}

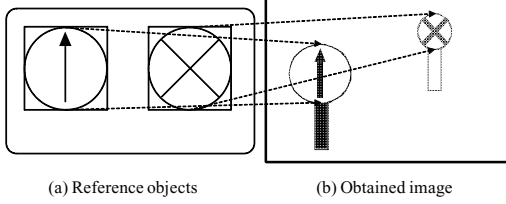


Figure 7. Parameter estimation using two reference objects.

where the image includes two traffic signs at different distances.

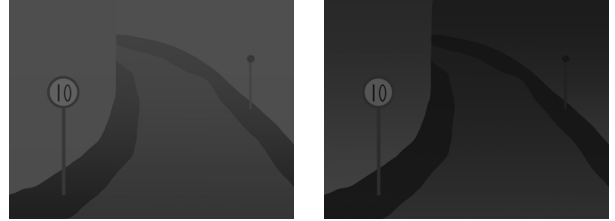
- **Extraction of traffic signs**
We detect two traffic signs in the input image referring to the database of traffic signs. In our experiment, though, we extracted the traffic signs manually.
- **Measurement of the distance**
The distance between the camera and traffic sign can be determined using the intrinsic parameters of the camera, the size in pixels of the traffic sign in the image, and the metric size of the traffic sign in the database. In our experiment, though, we measured the distance manually.
- **Estimation of the optical density and the maximum scattered light**
We estimated the optical density and maximum scattered light from the information of the two extracted traffic signs employing the Levenberg–Marquardt method. The initial value we use for Levenberg–Marquardt method is $A_{\infty}^{\parallel} = A_{\infty}^{\perp} = 64$ for 8-bit camera and $\beta = \{(Z_1 + Z_2)/2\}^{-1}$.
- **Haze removal**
We computed the dehazed image and the depth map from the estimated optical density and maximum scattered light.

Figure 7 illustrates how the database and the input image are used in parameter estimation.

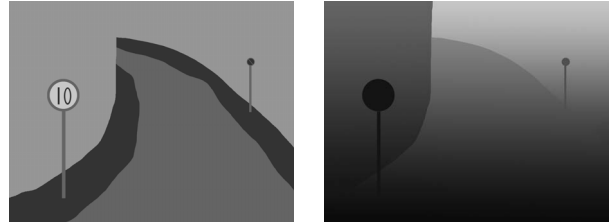
4. Experiments

4.1. Simulation results

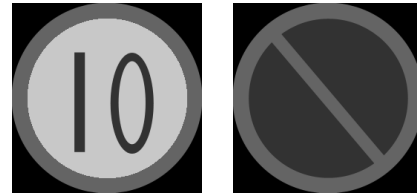
We conducted a dehazing simulation experiment. Figure 8 shows the generated input data for a hazy scene in the



(a) Observed light I^{\perp} (b) Observed light I^{\parallel}
Figure 8. Observed polarization images of the simulated scene.



(a) Object reflection R (b) Distance Z
Figure 9. True values used for simulation.



(a) Traffic sign 1 (b) Traffic sign 2
Figure 10. Database of two reference objects used in the simulation experiment.

simulation. Figure 8 (a) is the perpendicular component of the input light, and Fig. 8 (b) is the parallel component of the input light. Figure 9 is the true data used to generate the input image. Figure 9 (a) is light reflected by objects, and Fig. 9 (b) is the depth image. Figure 8 is generated from Fig. 9 in the simulation and parameters are set as $\beta = 0.1$, $A_{\infty}^{\parallel} = 20$, and $A_{\infty}^{\perp} = 80$.

We assume that the traffic-sign database is given; the database is shown in Fig. 10. In this experiment, the traffic sign recognition is recognized manually by the operator.

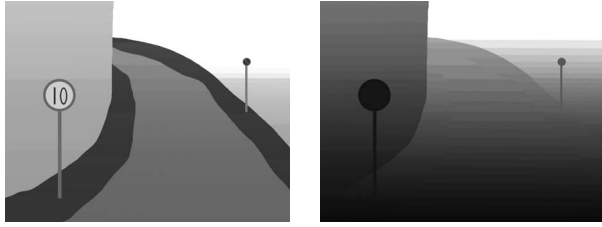
The DOP of the simulation scene is shown in Fig. 11. Brighter pixels represent a higher DOP. Figure 11 indicates that the DOP is high where the haze is dense.



Figure 11. Degree of polarization ρ in the simulated scene.



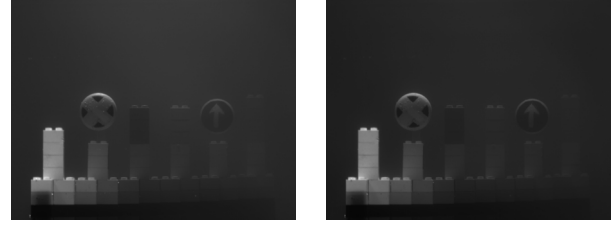
Figure 13. Polarization imaging camera.



(a) Computed object reflection R

(b) Distance Z

Figure 12. Experimental result of dehazing.



(a) Observed light I^\perp

(b) Observed light I^\parallel

Figure 14. Obtained polarization data for a real scene.

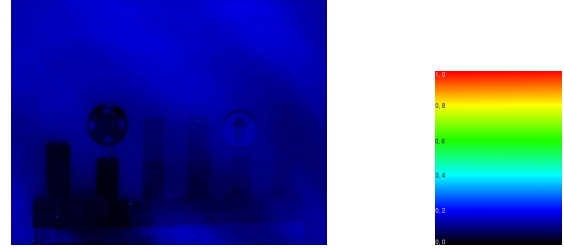
The optical density β and the maximum scattered light A_∞ are estimated employing the Levenberg–Marquardt method. The object light and the depth image are shown in Fig. 12 (a) and Fig. 12 (b), respectively, which are estimated from the input images (Fig. 8), the optical density β , and the maximum scattered light A_∞ .

Figure 12 (a) tells us that not only the haze of the traffic signs but also the haze of the road and objects is removed. However, the object light is not clearly estimated at far distance owing to the degradation of the object light contrary to the increase in the haze density.

4.2. Results for a real case

In this section, we present results for a real situation. Figure 13 shows the polarization imaging camera that we use to capture the polarization state of the scene. Figure 14 (a) is the perpendicular component of the scene brightness, and Fig. 14 (b) is the parallel component of the scene brightness. The DOP of the scene is shown in Fig. 15 for reference.

In our experiment, we mimic a hazy atmosphere and observe miniature traffic signs. Haze is caused by specular reflection at the surface of aerosols distributed in the atmosphere. The single-scattered light of the aerosols then partially polarizes. The arrangement of the camera and the traffic signs is illustrated in Fig. 16, a photograph of the experimental setup is shown in Fig. 17 (a), the arrangement of the toy blocks and the miniature traffic signs is shown in Fig. 17 (b), and the hazy scene generated by dissolving



(a) Degree of polarization ρ

(b) Gauge of pseudo-color

Figure 15. Degree of polarization in a real situation.

black paint in a water tank is shown in Fig. 17 (c). A white light mimics the sun and is set just above the water tank, orthogonal to the water surface so that the light is not polarized when penetrating the water. Figure 17 (c) shows that we can mimic the hazy scene by dissolving black paint in the water tank. This is because the light specularly reflects from the black particles distributed in the water.

Since we assume that the database of traffic signs is available, we use Fig. 18 for two reference objects. In our experiment, the traffic signs are recognized manually.

Table 2 presents the optical density β and the maximum scattered light A_∞ estimated employing the Levenberg–Marquardt method. The object light shown in Fig. 19 (a) and the depth map shown in Fig. 19 (b) are calculated from the input data shown in Fig. 14, the estimated optical density β , and the estimated maximum scattered light A_∞ . A detailed comparison made by magnifying the input image and the output dehazed image is shown in Fig. 20.

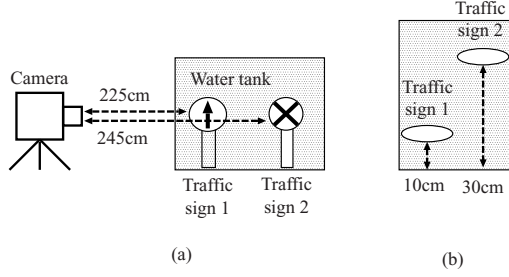


Figure 16. Geometric arrangement of the camera and two reference objects.

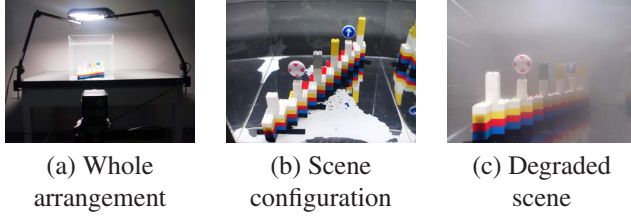


Figure 17. Experimental environment.

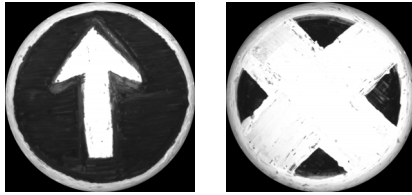


Figure 18. Database of two reference objects.

Table 2. Estimated value of maximum scattered light A_∞ and optical density β .

	Estimated value
Maximum scattered light A_∞^\perp	47.3
Maximum scattered light A_∞^\parallel	39.2
Optical density β	0.169

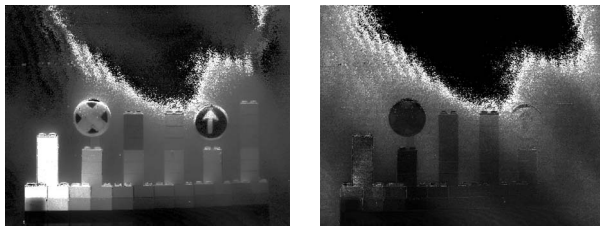


Figure 19. Dehazing result for the real scene.

Comparing Fig. 20 (a) and Fig. 20 (b), we see that the traffic sign and the toy blocks have become clear. The upper

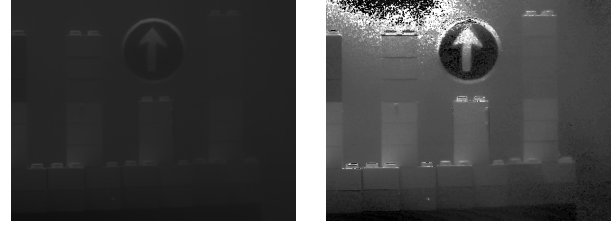


Figure 20. Comparison of the observed light and dehazing result.

region in Fig. 19 (a) is not well calculated since the scattering in the water tank does not occur over an infinite distance but over a finite distance. Another concern relating to the experimental result is the intense brightness of the closest toy block in Fig. 19 (a). We believe that this is explained by the experiment not fully reproducing the actual situation of an outdoor scene. It is speculated that the particles were not distributed uniformly, the particle size was too large or too small, the size of the water tank was too small, the reference object has specular reflection, the diffuse reflection of the object was too dark, the light was not illuminated uniformly, the distance of the light was not far enough, the incident angle of the light with respect to the object was not uniform, the reflection on the water surface or the transmission through the plastic tank affected the polarization state of the light, or that there was another reason for the discrepancy. Further investigation is needed to determine the actual reason.

5. Conclusion

We proposed a polarization-based method to estimate haze parameters from known information to improve visibility in poor weather. We tested the performance of our method both in simulation and for a real situation. Traffic signs were used in the experiments to demonstrate the applicability of our method in the field of intelligent transport systems.

In the experiment, the haze of the image was clearly removed over a large area; however, a portion of the haze was not removed owing to the difficulty of creating the same phenomena of haze in the laboratory.

We next intend to measure an actual hazy scene, which is a long-term plan since the chance of obtaining good data of haze is limited by weather. We also believe that dehazing is important in improving scattering underwater since it could assist in the navigation of vessels and submarines.

The most important work to carry out next is to improve the precision of the estimation. If we set the polarization imaging camera on top of a vehicle, we could capture a sequence of images. These images can include the same traffic sign at different distances since the vehicle is mov-

ing forward while capturing the sequence of images. Using this rich information, the estimation result is predicted to improve. We also plan to attempt to use reference objects other than traffic signs; for example, roads, vehicles, traffic signals, trees, and buildings.

Acknowledgments

This research was supported in part by the Grant-in-Aid for Scientific Research on Innovative Areas “Shitsukan” (no. 22135003) from MEXT, Japan, and in part by the Grant-in-Aid for Young Scientists (no. 24700176) from JSPS, Japan. The authors thank Masahito Aoyama for useful discussions. They also thank anonymous reviewers for their careful reviews of the paper.

References

- [1] M. Born and E. Wolf, *Principles of optics*, Pergamon Press, 1959. [1](#)
- [2] R. Fattal, “Single image dehazing,” *ACM Transactions on Graphics*, vol. 27, no. 3, pp. 72:1–72:9, 2008. [1](#)
- [3] K. He, J. Sun, and X. Tang, “Single image haze removal using dark channel prior,” *IEEE Transactions on Pattern Analysis and Machine Intelligence*, vol. 33, no. 12, pp. 2341–2353, 2011. [1](#)
- [4] E. Hecht, *Optics*, Addison-Wesley, 2002. [1](#)
- [5] S. G. Narasimhan and S. K. Nayar, “Chromatic framework for vision in bad weather,” in *Proceedings of IEEE Computer Society Conference on Computer Vision and Pattern Recognition*, pp. 598–605, 2000. [1](#)
- [6] Y. Y. Schechner, S. G. Narasimhan, and S. K. Nayar, “Polarization-based vision through haze,” *Applied Optics*, vol. 42, no. 3, pp. 511–525, 2003. [1](#)
- [7] Y. Y. Schechner and N. Karpel, “Recovery of underwater visibility and structure by polarization analysis,” *IEEE Journal of Oceanic Engineering*, vol. 30, no. 3, pp. 570–587, 2005. [1](#)
- [8] W. A. Shurcliff, *Polarized light: production and use*, Harvard University Press, 1962. [1](#)
- [9] S. Shwartz, E. Namer, and Y. Y. Schechner, “Blind haze separation,” in *Proceedings of IEEE Computer Society Conference on Computer Vision and Pattern Recognition*, pp. 1984–1991, 2006. [1](#)
- [10] R. T. Tan, “Visibility in bad weather from a single image,” in *Proceedings of IEEE Computer Society Conference on Computer Vision and Pattern Recognition*, 2008. [1](#)
- [11] T. Treibitz and Y. Y. Schechner, “Active polarization descattering,” *IEEE Transactions on Pattern Analysis and Machine Intelligence*, vol. 31, no. 3, pp. 385–399, 2009. [1](#)
- [12] L. B. Wolff and T. E. Boulton, “Constraining object features using a polarization reflectance model,” *IEEE Transactions on Pattern Analysis and Machine Intelligence*, vol. 13, no. 7, pp. 635–657, 1991. [1](#)